

THE IDENTIFICATION OF HIGHLY IONIZED METAL SPECIES IN THE HOT DA1 WHITE
 DWARF G191-B2B WITH THE *HUBBLE SPACE TELESCOPE*
 FAINT OBJECT SPECTROGRAPH

EDWARD M. SION

Department of Astronomy and Astrophysics, Villanova University, Villanova, PA 19085

RALPH C. BOHLIN

Space Telescope Science Institute, 3700 San Martin Drive, Baltimore, MD 21218

RICHARD W. TWEEDY

X-Ray Astronomy Group, University of Leicester, Leicester, UK LE1 7RH

AND

GERARD P. VAUCLAIR

Observatoire Midi-Pyrenees, CNRS URA285, F-31400 Toulouse, France

Received 1992 January 21; accepted 1992 March 3

ABSTRACT

Ultraviolet spectra of the hot DA white dwarf G191-B2B obtained with the *Hubble Space Telescope* and Faint Object Spectrograph have revealed a wide assortment of high-ionization metallic absorption features, many of which must be associated with the high gravity ($\log g = 7.55$) photosphere of this hot ($T_{\text{eff}} = 62,250$ K) degenerate. The most prominent highly ionized species is Fe v with several features or blends of features identified in the wavelength range 1320–1470 Å, implying an important role for Fe as a soft X-ray/EUV opacity source. The first detection in a DA white dwarf of the C III sextuplet $^3P^o\text{--}^3P$ appears as a broad trough with a width of about 3 Å and a central depth of 10%. The carbon abundance implied by this detection is consistent with the abundance implied by C IV, bolstering a photospheric origin for both ions. Absorption features of doubly and triply ionized silicon, oxygen, iron, and manganese are also tentatively identified, some of which are almost certainly associated with the DA photosphere or circumstellar environment. Based upon the nondetection of He II ($\lambda 1640$) to a limiting equivalent width of 50 mÅ, an upper limit hydrogen layer mass of $10^{-14} M_{\odot}$ is derived using a grid of stratified hot DA model atmospheres. Implications of our line detections for the problem of the soft X-ray/EUV opacity source in hot DA stars and for radiative forces theory and hot DA mass loss are briefly discussed.

Subject headings: diffusion — stars: abundances — white dwarfs

1. INTRODUCTION

The presence of heavy elements in the photospheres of hot hydrogen-dominated and helium-dominated white dwarfs implies that there are physical processes which counteract the expected downward gravitational diffusion on a time scale of tens of years for DA stars with $T_{\text{eff}} > 50,000$ K (Vauclair, Vauclair, & Greenstein 1979). If the radiative acceleration that is due to numerous EUV bound-bound transitions near the Planckian peak of the hot DA star exceeds the surface gravity, then heavy elements can be levitated at the photosphere in observable abundances or can even be expelled from the star via a selective ion outflow (Vauclair 1989 and references therein). Some kind of outflow is required to reduce the hydrogen layer masses in DA stars to values below $10^{-8} M_{\odot}$, in order to be consistent with the theoretical nonradial g -mode pulsation calculations and the observed blue and red edges of the ZZ Ceti instability strip (Winget & Fontaine 1982). However, stellar evolution calculations predict that the hydrogen layer mass remaining after the post-AGB evolution of hydrogen-burning planetary nuclei should be of order $10^{-4} M_{\odot}$ (Iben 1984 and references therein). The spectroscopic detection of trace metals may bear directly upon the question of whether white dwarfs lose mass. Even though the effect of line blanketing is less than 1% in any 20 Å band longward of the Lyman limit, the presence of many trace metals with abun-

dances too small for line detections may explain the soft X-ray/EUV opacity of hot DA stars like G191-B2B (Jordan et al. 1987; Paerels & Heise 1989) and Feige 24 (Vennes et al. 1989) without invoking helium as the principal EUV opacity source.

The hot DA1 white dwarfs G191-B2B and Feige 24 are the only H-rich degenerates with metal features that are suspected to be photospheric (Bruhweiler & Kondo 1981, 1983; Dupree & Raymond 1982). While Feige 24 is a close (but detached) binary with a chromospherically active M dwarf companion, G191-B2B has a common proper motion companion at a separation so large that accretion is extremely unlikely to complicate interpretations of surface metals (Sion & Starrfield 1984). Several recent developments underscore the critical importance of G191-B2B. Reid & Wegner (1988) have reported the detection of an H α emission core centered on the broad Balmer absorption line and have found an error in the systemic velocity of Trimble & Greenstein (1972). The new systemic radial velocity brings the velocity of the H α emission core ($+18 \text{ km s}^{-1}$) into apparent agreement with the velocity of the C IV, Si IV, and N V resonance absorption lines detected by Bruhweiler & Kondo (1981) with the *IUE* echelle. More recently, Bruhweiler & Feibelman (1991) report the detection of O V and O IV, as well as several lines of Fe V and Fe VI in G191-B2B, based upon their co-addition of two *IUE* echelle spectra. The velocities of these features appear to be in agree-

ment with the velocity of the Balmer and high-ionization metal lines.

In this *Letter*, new line identifications are based upon spectroscopic observations of G191-B2B obtained with the Faint Object Spectrograph (FOS) of the *Hubble Space Telescope* as part of the science verification program. These results are compared with recent line identifications in a co-addition of five point-source echelle spectra of G191-B2B from the SWP camera on *IUE* (Tweedy 1991). In § 2, we describe the details of the FOS instrumental setup, observations, and the line measurements. Section 3 contains the implications of our line identifications and summarizes the scientific results.

2. OBSERVATIONS

The hot DA1 white dwarf G191-B2B was observed with the FOS (Ford & Hartig 1990) in 1990 October on the red Digicon and in 1991 January on the blue Digicon. Five of the high-dispersion gratings were used to cover the spectral region 1140–6800 Å at a nominal resolving power of $R = 1300$. The 1 inch (2.5 cm) circular aperture was used for all observations. No flat-field correction to the observations are made; however, the reality of many features can be confirmed from the lack of any corresponding feature in the high S/N spectrum of 3C 273 (Bahcall et al. 1991).

3. LINE IDENTIFICATIONS

The weakest lines selected for measurement have equivalent widths of roughly 50 mÅ. All apparent absorption features with equivalent widths of at least 50–75 mÅ are regarded as candidates for real line absorption. In a few cases, features which looked *real* relative to the adjacent continuum are noted in this *Letter* despite having measured equivalent widths less than 50 mÅ. The cutoff of roughly 50 mÅ allows for the possi-

bility of errors in continuum placement and for the 10 times greater sensitivity but 10 times lower resolution of the FOS relative to the *IUE* echelle.

All potential features are measured using IRAF. Single or multiple Gaussian profiles are fitted with the routine SPLOT to obtain central wavelengths and equivalent widths. The uncertainty in equivalent width determinations is at least 20%, due largely to the difficulties in continuum placement. Sources for the line identifications include the extensive compilation of Kelly & Palumbo (1973), the new published UV line atlas of Morton (1991), the line atlas of Dean & Bruhweiler (1985) for hot sdO stars, the compilation of Fe v, Fe vi, and Fe vii laboratory transitions of Ekberg (1975, 1981), and the extensive tabulation of line identifications in Wolf-Rayet spectra by Willis et al. (1986). The important line identifications are described below and presented in Tables 1 and 2. Features having the most uncertain equivalent widths or those features weaker than 50 mÅ are indicated with a colon symbol and should be regarded with caution.

First, we have discovered the C III sextuplet $^3P^o-P$ with all six members of multiplet 4 contributing to a broad blended feature centered at 1175 Å. This feature is shown in Figure 1 and has an equivalent width of 250 mÅ \pm 20%. The C III absorption is undetected in G191-B2B by the *IUE*, because of the low sensitivity of the SWP echelle. Second, the presence of very highly ionized species, principally Fe v, are detected as single resolved features or as very strong blends of individual Fe v features (Table 1). The strongest and most numerous transitions of Fe v are identified in the wavelength range 1320–1470 Å. In Figure 2, two strong Fe v blended features at 1364 Å and 1375 Å are displayed. Since the FOS data on 3C 273 reveals a slope change in the continuum near this region, the appearance of these broad absorptions coincident with

TABLE 1
TENTATIVE Fe V LINE IDENTIFICATIONS

Measured Wavelength (Å)	E.W. (mÅ)	Laboratory Wavelength (Å)	Comments
1277.39	39:	Fe v 1276.876, 1277.077, 1277.316, 1278.291	
1321.277	35:	Fe v 1320.410, 1321.277, 1321.490	(Blend of three lines)
1329.888	42:	Fe v/Fe vi 1330.401	
1339.316	50	Fe v 1339.691	(Blend with O iv?)
1354.665	40:	Fe v 1354.847??	
1361.716	51	Fe v/Fe vi 1361.279–1361.825	(Blend of four lines)
1363.322	243	Fe v 1363.077–1363.376–1363.642, 1364.824, 1364.984, 1365.115	(Broad blend of six lines)
1366.968	44:	Fe v 1367.183??	
1371.766	30:	Fe v 1371.987/O v 1371.292	(Deep absorption blend)
1375.673	333	Fe v 1373.587, 1373.674, 1373.967, 1374.116, 1374.789, 1376.377, 1376.455, 1378.092, 1378.560	
1398.854	34:	Fe v 1397.106, 1397.753, 1397.972, 1400.243	
1402.4	107	Fe v 1402.388	(Blended with Si iv 1402.8)
1407.289	57	Fe v 1406.669, 1407.824, 1407.246	
1409.703	55	Fe v 1409.026, 1409.220, 1409.451	
1420.572	86	Fe v 1420.465	(Blended with an unidentified line at 1418.568)
1429.592	41	Fe v 1429.472	
1430.54	50	Fe v 1430.573	
1440.101	60	Fe v 1439.052, 1440.528 (Int. = 800), 1440.792	
1446.618	190	Fe v 1446.618 (Int. = 800), 1448.846 (Int. = 700)	Plus four weaker lines
1447.147	221	Fe v 1446.618, 1447.147	(Blend of two lines)
1455.88	120	Fe v 1454.701, 1455.559	(Blend of two lines)
1456.161	80::	Fe v 1456.161	
1465.388	393:	Fe v 1464.876?, 1465.383?	(Dominated by flat field artifact)

TABLE 2
OTHER PHOTOSPHERIC/CIRCUMSTELLAR FEATURES

Measured Wavelength (λ)	Ion	Multiplet Number	Comments
1176.08	C III	4	250 mÅ (six lines)
1190.336	Si III/Si II	1/5	Blend of two lines
1192.65	Si III/Si II	1/5	Blend of two lines
1197.667	Si III/Si II	1/5	Blend of two lines
1202.726	Si III	1	
1206.592	Si III	2	
1238.783	N V		100 mÅ
1243.276	N V		141 mÅ
1283.213	Mn III	9	
1287.245	Mn III	9	
1291.191	Mn III	9	
1299.596	Si III	4	
1339.316	O IV?		(Blend with Fe v?)
1343.675	O IV?		(Very weak)
1371.766	O V		Blend with Fe v
1394.075	Si IV		75 mÅ
1402.892	Si IV		107 mÅ
1548.439	C IV		180 mÅ
1551.063	C IV		97 mÅ
1584.367	O III		50 mÅ:
1587.052	O III		Blend of three O III lines
1768.154	O III		65 mÅ
			Blend of three O III lines
			1767.78 (Int. = 1000)
1612.163	C III		
1639.321	He II?		Too shortward-shifted for photosphere
1993.823	Fe III	50	Blend of three lines
1995.501	Fe III	50	Blend of three lines
1997.322	Fe III	50	Blend of three lines

strong (intensity = 800) Fe v features, may be artificially contaminated. Third, Table 2 includes tentative identifications for a number features of Si III, Mn III, O III, C III, and weak O IV, along with the previously discovered resonance doublets of N V, C IV, and Si IV. If all of these identifications are correct, then radiative support calculations will be required to demonstrate that their origin is due to levitation in the white dwarf photosphere versus formation in a circumstellar shell or the interstellar medium.

Despite the better resolution of the *IUE* echelle, the FOS detects a far richer line spectrum due to its higher sensitivity

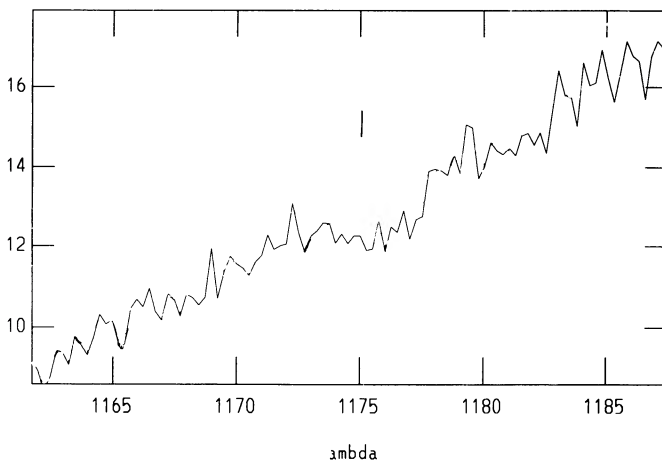


FIG. 1.—FOS counts vs. wavelength λ for the region of the broad C III sextuplet blend centered at $\lambda 1176.6$ and indicated with a tick mark.

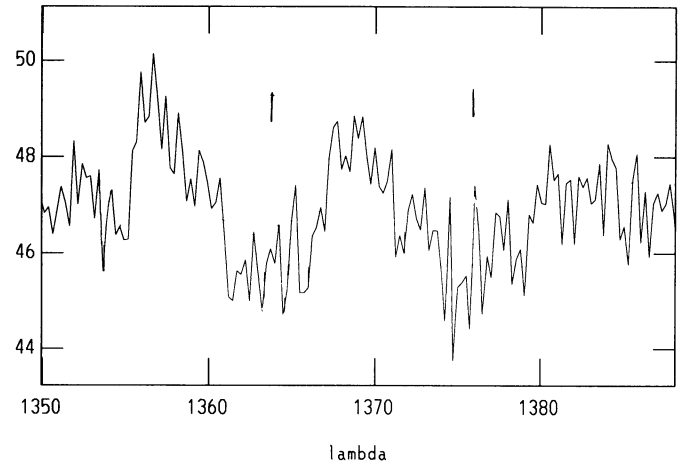


FIG. 2.—FOS counts vs. wavelength λ showing two of the strongest Fe v blends centered on $\lambda 1364$ and $\lambda 1376$. The broad emission bump centered at $\lambda 1356$ is a flat-field artifact. The approximate centers of the two Fe v blends are indicated with tick marks.

and S/N (2.4 m telescope vs. 0.45 m). While the detection of the narrowest lines identified with the *IUE* echelle was not possible with FOS, the higher sensitivity of FOS enables the detection of broader and shallower features. When *IUE* and FOS both detect a feature the equivalent widths agree within a factor of two. Some examples of FOS and *IUE* measurements are presented in Table 3.

4. IMPLICATIONS

Our FOS line identifications in Tables 1 and 2 hold important implications for many of the above issues in the following ways.

1. Our first detection of the C III sextuplet in G191-B2B implies that $\log [N(C)/N(H)] > -6$ according to the theoretical UV line profile grid of Henry, Shipman, & Wesemael (1985), whereas the nondetection of C III with the *IUE* echelle implied $\log [N(C)/N(H)] < -6$, based upon the metal abundance calculations of Vennes, Thejll, & Shipman (1991). The carbon abundance implied by the detection of C IV ($\log [N(C)/N(H)] = -5.6$) would no longer be discrepant with the upper limit carbon abundance set by the nondetection of C III. Therefore, the ionization balance would be closer to Saha-Boltzmann and would bolster a photospheric origin for the C III and C IV.

2. The spectrum of Fe v with numerous lines or blends provides the most important data base for testing recent theoretical radiative acceleration calculations on iron. The radiative acceleration on iron ions in the frequency interval $d\nu$ due to the

TABLE 3
COMPARISON OF FOS AND *IUE* EQUIVALENT WIDTHS

Ion	FOS (mÅ)	<i>IUE</i> (mÅ)
Si II $\lambda 1260$	68	86
N I $\lambda 1200$ triplet ..	91 (blend of 3)	150 (total of three lines)
C II $\lambda 1334$	54	111
C IV $\lambda 1548$	180	192
C IV $\lambda 1551$	97	151
Si IV $\lambda 1394$	75	82
Si IV $\lambda 1402$	107	72

momentum transferred by the outgoing radiation flux is given by

$$g_{\text{rad},v} dv = (4\pi/c)[1/X(\text{Fe})]k_v(\text{Fe})H_v dv,$$

where $X(\text{Fe})$ is the mass fraction of iron, $k_v(\text{Fe})$ is the iron contribution to the monochromatic opacity, H_v is the Eddington flux, and c is the speed of light. Chayer, Fontaine, & Wesemael (1991) have presented detailed computations of the radiative acceleration on Fe, from which equilibrium abundance profiles of Fe are obtained. Chayer et al. (1991) demonstrate that in the absence of other competing mechanisms, detectable amounts of Fe would be visible at the photosphere of a $0.6 M_{\odot}$ DA white dwarf when $T_{\text{eff}} > 50,000$ K. When actual detailed abundance analyses of Fe are carried out, photospheric Fe abundances can be derived from the line strengths. The Fe v lines associated with G191-B2B arise from excited states at least 23 eV above ground, from the $3d^34s$ level instead of the $3d^4$ ground state (Ekberg 1975). Thus, Fe v is formed in a very hot, dense region and presents an even stronger case for a photospheric interpretation than the C iv, N v, and Si iv lines in Table 2. Moreover, Tweedy (1991) finds preliminary evidence from the coaddition of five *IUE* echelle spectra that the velocities of five strong, unblended Fe v lines are incompatible with the velocities of N v and C iv, the latter being shortward-shifted by ~ 10 km s $^{-1}$. Fe v and Fe vi emission is found in Wolf-Rayet winds out to 5 stellar radii (Koenigsberger 1990) suggesting that a hot, dense shell could also be a plausible formation region for these lines.

3. The variety of trace metallic elements of doubly ionized Mn, O, Fe, Si, N, and Ni that are detected with the FOS and with the *IUE* echelle (Bruhweiler & Feibelman 1991) also lends support to the idea that a host of trace metals in hot DA photospheres may be providing the soft X-ray/EUV opacity (Vennes et al. 1989). In this case, helium would not be needed as the source of EUV/X-ray opacity.

4. The appearance of a weak absorption feature near 1640 Å raised the possibility of weak He ii in G191-B2B; but the feature is too shortward-shifted (1639.321) to make this identification plausible. We note that Vennes et al. (1988) predict that in a 60,000 K DA star, helium can be radiatively supported in detectable surface abundance. The absence of He ii in the FOS spectrum does provide an important upper limit constraint to the hydrogen layer mass such that He ii would not be detected. Using a grid of stratified H/He model atmospheres by

Finley (1991) for $T_{\text{eff}} = 62,000$ K and $\log g = 7.5$ as the parameters of G191-B2B, the nondetection of He ii (1640) to the FOS limit of 50 mÅ implies $M_h = 10^{-13.95} M_{\odot}$ (Finley 1991). This H layer mass is just barely smaller than the value $\log M_h = -13.85$ above which all He lines disappear.

Given the variety of ionization states of metals detected, it is possible to make a preliminary comparison of them with theoretical predictions of abundances and expected ionization fractions of these species for a hot DA white dwarf with $\log g = 8$, $T_{\text{eff}} = 60,000$ K. Radiative forces/diffusion calculations for CNO and Si only, have been carried out for G191-B2B by one of us (G. V.) and predict the following abundances and ionization fractions at optical depth 0.1: C/H = 1.5×10^{-5} with C iii 9%, C iv 78%, C v 9%; N/H = 10^{-5} with N iii 23%, N iv 76%, N v 0.5%; O/H = 4×10^{-6} with O iii 43%, O iv 56%, and O v 1.3%; Si/H = 3×10^{-6} with Si iii = 0.04%, Si iv 12%, Si v 88%. Note that all of these species are seen in the FOS data (except N iii, N iv, Si v, and C v). On the basis of the above theoretical results, it is surprising that Si iii and N v are present in detectable abundance and that N iii and N iv are absent or extremely weak. However, O v $\lambda 1371$ is very weak while O iii and O iv are present, which is compatible with the theoretical prediction. Abundance determinations of the observed ion species for comparison with further radiative forces/diffusion calculations are clearly needed.

In conclusion, the FOS spectra of the science verification object G191-B2B have revealed an important and varied assortment of high-ionization absorption lines associated with either the photosphere or a dense circumstellar environment. The line data we have reported should spawn renewed theoretical calculations of radiative forces on trace elements in hot DA atmospheres and the possible consideration of other physical processes (e.g., mass loss) operative at high gravity.

We thank G. Hartig for his inexhaustible patience in helping us understand the subtleties of the FOS and for his aid with accessing all of the relevant sets of FOS calibration data. Cautions from the FOS flat field experts, B. Margon and S. Anderson, were very helpful. We thank C. R. Ready for assisting with the line measurements. This work was supported by NASA grant NAG 5-1630 to the FOS team. One of us (E. M. S.) is grateful for a 6 month sabbatical visit supported by STScI. Participation by E. M. S. was also supported by NSF grant AST90-16283 to Villanova University.

REFERENCES

- Bahcall, J. N., Jannuzi, B. T., Schneider, D. P., Hartig, G. F., Bohlin, R. C., & Junkkarinen, V. 1991, *ApJ*, 377, L5
 Bruhweiler, F. C., & Feibelman, W. 1991, preprint
 Bruhweiler, F. C., & Kondo, Y. 1981, *ApJ*, 248, L123
 ———. 1983, *ApJ*, 269, 657
 Chayer, P., Fontaine, G., & Wesemael, F. 1991, in *White Dwarfs*, ed. G. Vauclair & E. Sion (Dordrecht: Kluwer), 249
 Dean, C. A., & Bruhweiler, F. C. 1985, *ApJS*, 57, 133
 Dupree, A. K., & Raymond, J. 1982, *ApJ*, 263, L63
 Ekberg, J. O. 1975, *Phys. Scripta*, 12, 42
 ———. 1981, *Phys. Scripta*, 23, 7
 Finley, D. S. 1991, private communication
 Ford, H. C., & Hartig, G. 1990, *FOS Instrument Handbook*, Version 1.1 (Baltimore: STScI)
 Henry, R. B. C., Shipman, H. L., & Wesemael, F. 1985, *ApJS*, 57, 145
 Iben, I. 1984, *ApJ*, 277, 333
 Jordan, S., Koester, D., Wulf-Mathies, C., & Brunner, H. 1987, *A&A*, 185, 253
 Kelly, R. L., & Palumbo, L. J. 1973, *NRL Report 7599*
 Koenigsberger, A. 1990, *Astr. Ap. A&A*, 235, 282
 Morton, D. C. 1991, *ApJS*, 77, 119
 Paerels, F., & Heise, J. 1989, *ApJ*, 339, 1000
 Reid, N., & Wegner, G. 1988, *ApJ*, 335, 953
 Sion, E. M., & Starrfield, S. G. 1984, *ApJ*, 286, 760
 Tweedy, R. 1991, Ph.D. thesis, Univ. of Leicester
 Trimble, V., & Greenstein, J. L. 1972, *ApJ*, 177, 441
 Vauclair, G. 1989, in *White Dwarfs*, ed. G. Wegner (Berlin: Springer), 176
 Vauclair, G., Vauclair, S., & Greenstein, J. L. 1979, *A&A*, 80, 79
 Vennes, S., Chayer, P., Fontaine, G., & Wesemael, F. 1989, *ApJ*, 336, L25
 Vennes, S., Pelletier, C., Fontaine, G., & Wesemael, F. 1988, *ApJ*, 331, 876
 Vennes, S., Thejll, P., & Shipman, H. L. 1991, in *White Dwarfs*, ed. G. Vauclair & E. Sion (Dordrecht: Kluwer), 235
 Willis, A. J., et al. 1986, *ApJS*, 63, 417
 Winget, D., & Fontaine, G. 1982, in *Pulsations in Classical and Cataclysmic Variable Stars*, ed. J. P. Cox & C. J. Hansen (Boulder: JILA), 46